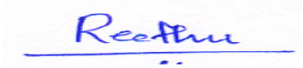



# Automation of Complex Power Systems

## Project Report

### Simulation and Test of Micro-grid Dynamics

Submitted by

Matriculation Number	Name	Signature	Date
376234	Reethu Mariam Raphael		12.08.2019
383702	Md Nahid Hossain Khan		12.08.2019



## Contribution

➤ Reethu Mariam Raphael:

- Prepared the Introduction, Literature review, Converter Control and Preliminary Conclusions as part of the report.
- Calculated the controller gains for the voltage control loop and document the same in the report.
- Prepared simulink model for both Grid Supporting Converters operating as current source and operating as voltage source and analyzed the results.

➤ Md Nahid Hossain Khan:

- Calculated the controller gains for the current control loop and document the same in the report.
- Prepared simulink model for one microgrid with Grid forming converter and other as Grid Supporting Converter operating as current source
- Analyzed the simulated output and documented it in the report.

## Table of Contents

No.	Content	Page No.
1.	Introduction	4
2.	Literature Review	5
2.1	Microgrid	5
3.	Converter Control	5
3.1	Power Converters	5
3.2	Control Structure	6
3.2.1	Grid-supporting controller acting as Current Source Inverter (CSI)	6
3.2.2	Grid-supporting controller acting as Voltage Source Inverter (VSI)	7
3.2.3	Grid-forming controller acting as Voltage Source Inverter (VSI)	8
3.3	Preliminary Conclusions	8
4.	Controller Design Procedures	9
4.1	Basic Elements	9
4.2	Grid-Forming Controller	12
4.2.1	Voltage Control Loop	12
4.2.2	Current Control Loop	12
4.3	Grid-Supporting Controller	12
4.3.1	Droop Control	12
4.3.2	Power Control Loop	12
4.3.3	Current Control Loop	12
5.	Simulink Model	13
6.	Simulation Result, Analysis and Conclusion	17
7.	References	20

## 1. Introduction

The aim of this project is to understand and analyze the dynamics of a microgrid model operating in islanding mode, with focus on the role played by the local controller using droop principle.

This report gives a detailed overview of the control philosophy, control structure used, design of controllers, Simulink model, output of the models and an analysis of the results obtained.

### Requirements:

The proposed microgrid model includes the following components:

- 2 local energy sources each represented by a constant DC voltage source of 750 V
- 1 variable resistive load with nominal value of 50 Ohm

The nominal grid characteristics are:

- phase voltage of 220V
- rated frequency 50Hz.

For each DG, the requirements included at the output:

- Three phase inverters operating at 10 kHz switching frequency;
- Converter is controlled by means of nested loop architecture
- LCL filter with
  - inductance  $L_{F1}$  of 3mH (inverter side)
  - capacitance  $C_F$  of 10 $\mu$ F
  - inductance  $L_{F2}$  of 1.5mH (grid side)

The parameters of the three-phase line connecting the LCL filter to the variable resistive load are:

- $R=1\Omega$
- $L=10\text{mH}$

## 2. Literature Review

Since the early 2000s, there has been an increasing growth in the field of microgrids with the development in the approaches used for the integration of renewables into the power systems. The enabling of ac microgrids in distribution networks not only allows delivering distributed power but also providing grid support services during regular operation of the grid, as well as powering isolated islands in case of faults and contingencies and thereby increasing the performance and reliability of the electrical system [1]. The control technique proposed in the IEEE paper titled “Control of Power Converters in AC Microgrids” [1] has been used as the main reference for this project. An overview of the different terms that are used throughout this report is given below:

### 2.1 Microgrid

A microgrid is a localized group of distributed energy sources and interconnected loads, within clearly defined electrical boundaries, that typically operates connected to and synchronous with the traditional centralized grid (macro grid). A microgrid can connect and disconnect from the grid to enable it to operate in both grid-connected and island-mode.[2] .The microgrid consists of a hierarchical control that can manage the operation in the two modes and the central controller oversees the conditions required to switch between modes.

In grid-connected mode, the microgrid supplies or draws power from the utility grid depending on the generation and load demand. In case of an emergency or power shortage, power interruption takes place and the microgrid shifts to islanded mode of operation.[3]. The microgrid operates only in islanded mode in this project. Hence, the voltage  $E$  and the frequency  $\omega$  must be maintained at nominal values of 220V (phase voltage) and 50Hz respectively to ensure that the hierarchical structure allows to manage the dynamics of the microgrid in the islanded mode whereas the central controller is not considered in this mode of operation.

## 3. Converter Control

### 3.1 Power Converters

Based on the operation in an ac microgrid, power converters can be classified into mainly 3 types : grid-forming, grid-feeding and grid-supporting power converters[5] [6].

- Grid-forming Converter: It is represented as an ideal AC voltage source with low-output impedance, setting the voltage  $E$  and the frequency  $\omega$  of the microgrid [1].
- Grid-feeding Converter: It is designed to deliver power to an energized main grid, represented by an ideal current source connected to the grid in parallel with an impedance. The current source must be perfectly synchronized with the AC voltage at the connection point in order to regulate active and reactive power exchanged with the grid [1].
- Grid-supporting Converter: It can be represented as an ideal AC-controlled current source in parallel with a shunt impedance or an ideal AC voltage source in series with a link impedance. This converter regulates its output current/voltage to keep the value of the grid frequency and voltage close to their rated values [1].

A grid-feeding power converter requires either a generator or a power converter to form the grid voltage to operate and therefore it cannot operate independently in island mode. Whereas a grid forming power converter usually operates in islanded mode, since in the main grid the ac voltage is conventionally

formed by synchronous generators [4]. A grid-supporting power converter is in between a grid-feeding and a grid-forming power converter. If it is implemented as a current source, it needs at least one grid former to operate, whereas if it is controlled as a voltage source with link impedance, it can operate in both grid-connected and island mode [1].

Therefore, from the above information it can be concluded that the microgrid model of this project should include either grid-forming or grid-supporting converter and its control.

## 3.2 Control Structure

Based on the conclusions from the previous section, three configurations namely grid-supporting converter acting as current source, grid-supporting converter acting as voltage source and grid-forming converter acting as voltage source were modelled according to [1]. Each one of them were initially tested with a single DC voltage source and then with two DC voltage sources.

### 3.2.1 Grid-supporting controller acting as Current Source Inverter (CSI)

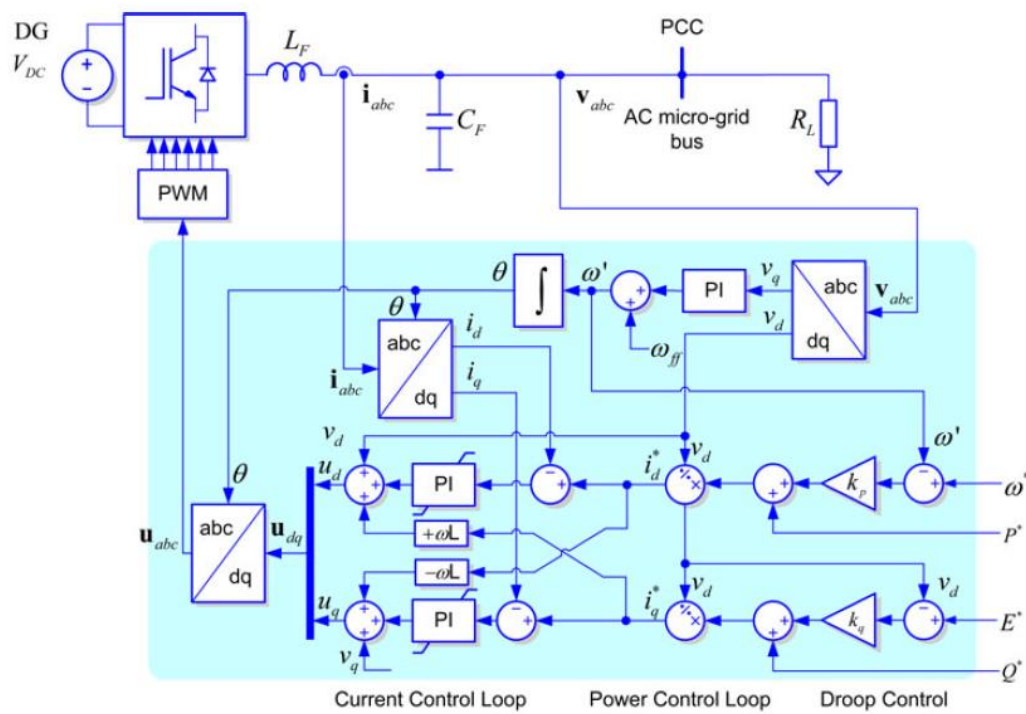


Figure.1 Basic control structure of three-phase grid-supporting power converters operating as a current source [1]

A grid-supporting power converter is controlled as a current source (fig.1) with a parallel impedance. Its main objective is not only to supply the load connected to the microgrid, but it should additionally be adjusted to contribute to regulate the voltage amplitude and frequency of both the AC grid and the microgrid [1].

Using the dq-transform, the voltages  $v_d$ ,  $v_q$  from the measuring point on the microgrid, the measured frequency and  $\theta$  from  $v_q$  through the PI controller and the currents  $i_d$ ,  $i_q$  from the measuring point on the microgrid were obtained. The inductance on the converter side  $L_{F1}$  and the capacitance  $C_F$  of the LCL filter at the output of the power converter are considered as the measuring points for the measured current  $i$  and measured voltage  $v$  respectively.

Using this information, the controls such as droop control, power control and current control were applied. In Droop Control, to make the required correction on the measured active power  $P$ , the variance between the measured frequency and the nominal frequency is used as input. Whereas in Power Control, to obtain  $i_d^*$  and  $i_q^*$  based on  $v_d$ ,  $v_q$  from the respective measuring points, the required values of  $P^*$  and  $Q^*$  given at the output of the droop control are used. In Current Control, the inputs to the PI current controller are variance between the required values  $i_d^*$  and  $i_q^*$  and the measured values  $i_d$ ,  $i_q$ . The output voltage  $u_{dq}$  is transformed back to 3-phase  $u_{abc}$  and fed into the PWM of the power converter. The reference values  $P^*$  and  $Q^*$  are required to establish the  $P^*$  and  $Q^*$  from the variance  $\Delta P$  and  $\Delta Q$  provided by the droop control.  $P^*$  and  $Q^*$  are calculated based on the nominal voltage  $E$  and variable resistive load value. The frequency and angle integrator are replaced with a Phase-Locked Loop (PLL) unit in order to eliminate the PI set of unknowns.

### 3.2.2 Grid-supporting controller acting as Voltage Source Inverter (VSI)

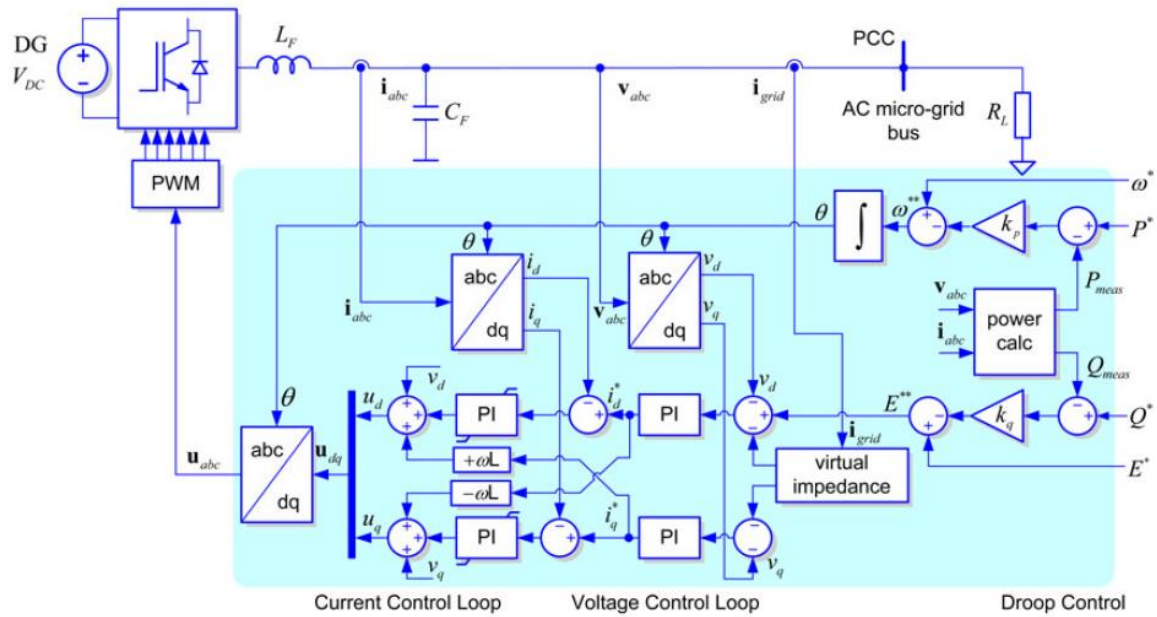


Figure.2 Basic control structure of three-phase grid-supporting power converters operating as a Voltage source [1]

A grid-supporting power converter is controlled as a voltage source with a link impedance. Here, the measured values  $P$  and  $Q$  are obtained directly from a measuring bloc using 3-phase  $u_{abc}$  and  $i_{abc}$  as the inputs. The variance between the measured active power  $P$  and reactive power  $Q$  and the required active power  $P^*$  and reactive power  $Q^*$  is used as the droop control input to get the correction required on the frequency and the voltage  $v_d^*$ . The correction is based on the nominal values of frequency  $\omega$  and voltage  $E$ .

Using the dq-transform, the voltages  $v_d$ ,  $v_q$  from the measuring point on the microgrid and currents  $i_d$ ,  $i_q$  from the measuring point on the microgrid are obtained. The inductance on the converter side  $L_{F1}$  and the capacitance  $C_F$  of the LCL filter at the output of the power converter are considered as the measuring points for the measured current  $i$  and measured voltage  $v$  respectively. The inputs to the voltage control loop are the measured voltage values of  $v_d$  and  $v_q$ . The measured voltage value  $v_q$  is expected to stay close to 0. Hence, the voltage  $v_d$  is set based on the droop control applied to the reactive power  $Q$ . The currents  $i_d^*$  and  $i_q^*$  constitute the voltage controller outputs and the inputs to the PI current controller are the variance between the required currents  $i_d^*$  and  $i_q^*$  and the measured currents  $i_d$ ,  $i_q$ . The output voltage  $u_{dq}$  is transformed back to 3-phase  $u_{abc}$  and fed into the PWM of the power converter.

Additionally, there is a virtual impedance included in the design which is intended to enhance voltage stability of the microgrid by establishing a constant impedance, based on which the required voltage is calculated. At any given time, the voltage controller inputs must be stabilized independent of grid load.

### 3.2.3 Grid-forming controller acting as Voltage Source Inverter (VSI)

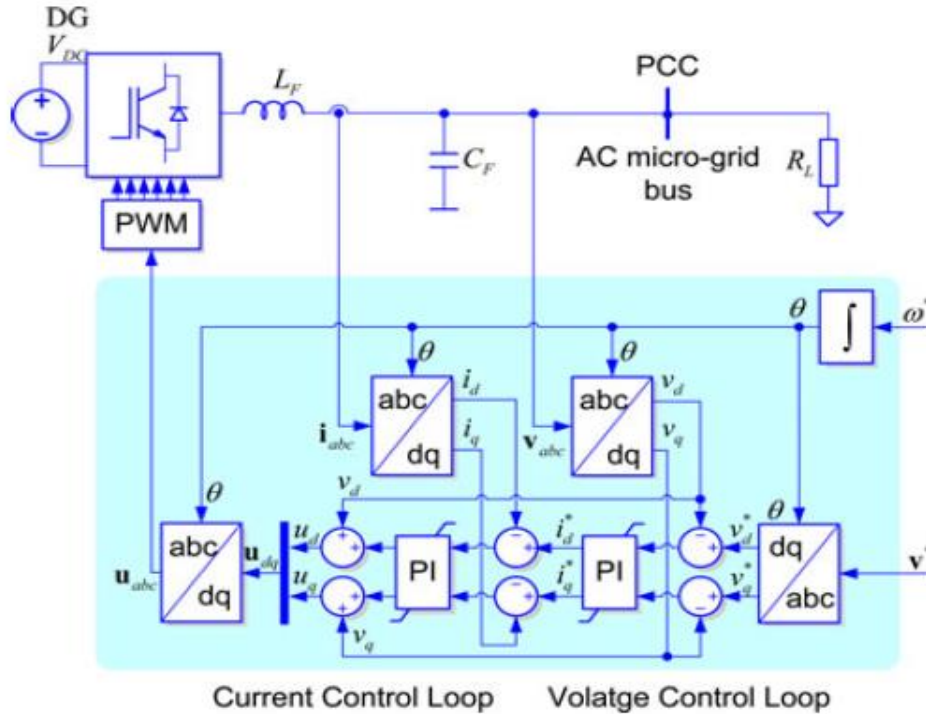


Figure.3 Basic control structure of three-phase grid-forming power converters operating as a Voltage source [1]

The grid-forming power converters (fig.3) are controlled in closed loop to work as ideal ac voltage sources with a given amplitude  $E$  and frequency  $\omega$ . Since it presents a low-output impedance, it needs accurate synchronization system to operate in parallel with other grid forming converters [1]. In the outer loop, the measured voltage is controlled against the reference value and in the inner loop, the measured current is controlled based on the required voltage. The voltage of the capacitor  $C_F$  is the measuring point for the measured voltage  $v$ . The charged capacitor  $C_F$  (charged by controlled current) keeps the output voltage equal to the reference voltage.

### 3.3 Preliminary Conclusions

Each one of the configurations mentioned were initially tested with a single DC voltage source and then with two DC voltage sources in Simulink.

The power and current controllers were designed based on the literature. The voltage controller constants were chosen in the same way.

Stable outputs value within the range of the reference for voltage and frequency can be seen for both the grid-supporting controller functioning as CSI and grid-forming controller functioning as VSI.

In figure 1, the grid-supporting controller functioning as VSI, comprises more controller constant for Virtual Impedance which makes the grid-supporting controller as most robust among three configurations [1].



The grid-supporting controller having low-impedance and functioning as VSI, resulting the output active and reactive power to the microgrid is influenced by the AC grid voltage, source and the link impedance.

If a Virtual Impedance replaces the link impedance, the grid-supporting controller can govern the voltage  $E$  and frequency  $\omega$  at the connection point in both parallel and islanded microgrid modes without needing a grid-forming converter.

Therefore, the microgrid controller was designed based on the following configuration:

- According to the figure 3 above, the first DG or local energy source is connected to a grid-forming controller functioning as voltage source inverter (VSI);
- A grid-supporting controller functioning as current source inverter (CSI) is connected to the second DG or local energy source.

The following sections of this report illustrates procedures for designing controller, the Simulink model, the Simulation results, analysis and conclusion of this configuration.

## 4. Controller Design Procedures

## 4.1 Basic Elements

LC filter is considered instead of LCL filter to evaluate the system as a 2<sup>nd</sup> order system. Even though connecting the inductor near the point of common coupling (PCC) as a part of line inductance lead to dropping in voltage, this can easily compensate by considering a higher voltage across the capacitor.

The inner control bandwidth of the PWM signal generator is very high compared to the outer voltage loop control loop. We considered the PWM signal generator is in ideal condition with infinite bandwidth. For analyzing the outer voltage loop, the delays of inner loop can be ignored.

The controller block diagram is given below.

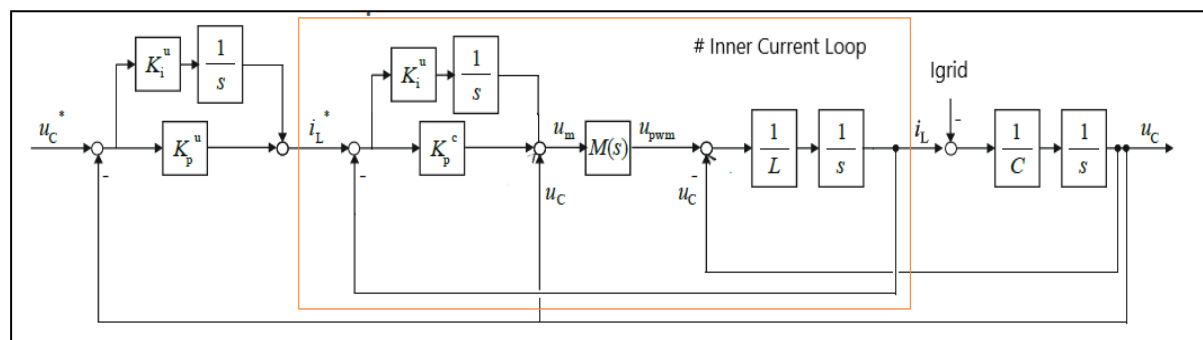


Figure. 4 Controller Block Diagram [7]

### I. Inner Control Loop

The transfer function for the inner current loop can be calculated by equation 1 as follows:

$$\frac{i_L}{u_M} = \frac{\frac{1}{Ls}}{1 + \frac{1}{Ls} \cdot (K_p + \frac{K_i}{s})} \dots \dots \dots (1)$$

The stiffness function is referred as disturbance rejection ability function is shown in equation 2, 3, and 4.

$$S(s) = \frac{u_M}{i_L} = K_p + \frac{K_i}{s} + Ls \dots \dots \dots (2)$$

$$S(j\omega) = K_p + j(\omega L - \frac{K_i}{\omega}) \dots \dots \dots (3)$$

$$\left| \frac{I_{grid}(j\omega)}{U_c(j\omega)} \right| = \sqrt{K_p^2 + (\omega L - \frac{K_p}{\omega})^2} \dots \dots \dots (4)$$

## II. Outer Voltage Control Loop

The transfer function for the outer voltage control loop is illustrated in equation 5.

$$\frac{U_c}{I_{grid}} = \frac{\frac{1}{Cs}}{1 + \frac{1}{Cs} \cdot (K_p + \frac{K_i}{s})} \dots \dots \dots (5)$$

Equation 6, 7 and 8 are showing the stiffness function for voltage control loop.

$$S(s) = \frac{I_{grid}}{U_c} = K_p + \frac{K_i}{s} + Cs \dots \dots \dots (6)$$

$$S(j\omega) = K_p + j(\omega C - \frac{K_i}{\omega}) \dots \dots \dots (7)$$

$$\left| \frac{I_{grid}(j\omega)}{U_c(j\omega)} \right| = \sqrt{K_p^2 + (\omega C - \frac{K_p}{\omega})^2} \dots \dots \dots (8)$$

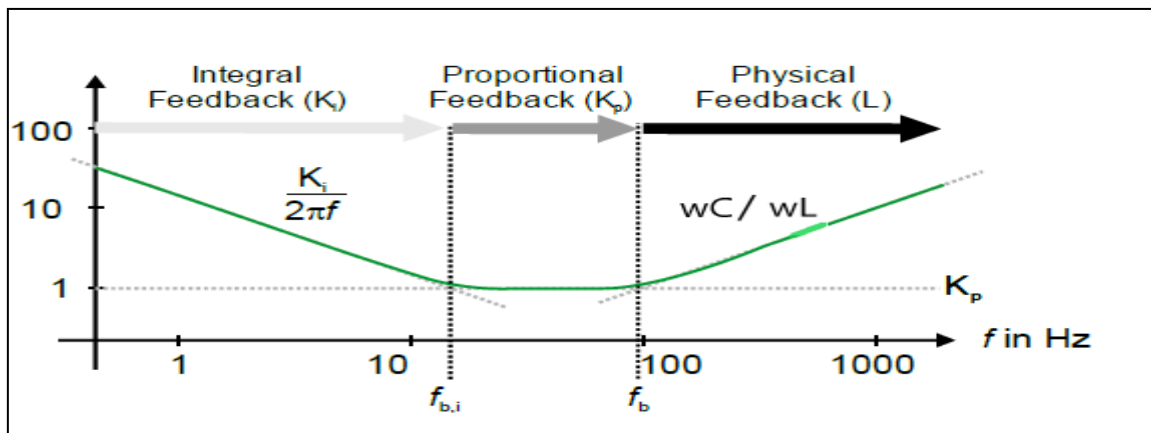


Figure.5 Cut-off frequencies of Dynamic Stiffness [7]

Figure. 5 Explains the method of Dynamic Stiffness for calculating cut-off frequency/controller gains.

Here,

$f_{b,i}$  = Corner frequency until which Integral Gain is dominant in determining stiffness

$f_{b,i}$  = Corner frequency until which Proportional Gain is dominant in determining stiffness

Region 1: Integral Feedback  $\omega \ll \omega_{b,i}$

$$|S(j\omega)| = \frac{K_i}{\omega} \dots \dots \dots (9)$$

Region 2: For Proportional Feedback  $\omega_{b,i} < \omega < \omega_{b,p}$

$$|S(j\omega)| = K_p \dots \dots \dots (10)$$

Region 3: For Physical Feedback  $\omega_{b,i} < \omega < \omega_{b,p}$

$$|S(j\omega)| = \omega C / \omega L \dots \dots \dots (11)$$

The proportional state feedback bandwidth is chosen far lower than the modulator bandwidth for ensuring desired system dynamics. This enables us to ignore the modulator dynamics and use the simplified frequency response function. Eigenvalues of the system are characterized into faster and slower types in the nested loop solution which lead the problem to be evaluated into three simpler steps namely current loop, voltage loop, and power delivery loop.

By considering the rule of thumb, the required proportional state feedback gain is selected.

$$K_p = 2\pi \cdot \frac{f_{PWM}}{10} \cdot L \text{ or } K_p = 2\pi \cdot \frac{f_{PWM}}{10} \cdot C \dots \dots \dots (12)$$

The system has been designed considering the dominant pole of the inner current loop which is one decade slower than the inner loop. So, with reference to PWM generator frequency, controller gains for outer voltage control loop is determined.

### **Controller gains calculation**

a) Current Control Loop

$$f_{k,p} = \frac{f_{PWM}}{10} = 1000 \text{ Hz}$$

$$f_{k,i} = \frac{f_{k,p}}{10} = 100 \text{ Hz}$$

$$K_p = 2 \cdot \pi \cdot f_{k,p} \cdot 3mH = 18.84 \Omega$$

$$K_i = 2 \cdot \pi \cdot f_{k,i} \cdot K_p = 11843.52 \Omega$$

b) Voltage Control Loop

$$f_{k,p} = \frac{f_{PWM}}{10} = 1000 \text{ Hz}$$

$$f_{k,i} = \frac{f_{k,p}}{10} = 100 \text{ Hz}$$

$$K_p = 2 \cdot \pi \cdot f_{k,p} \cdot 10\mu F = 0.0628 \Omega^{-1}$$

$$K_i = 2 \cdot \pi \cdot f_{k,i} \cdot K_p = 11843.52 \Omega^{-1}$$

## 4.2 Grid-Forming Controller

### 4.2.1 Voltage Control Loop

The outer voltage control loop uses the values of voltage and frequency which are maintained in the grid as inputs. Equation 13 and 14 shows relevant formulas.

$$i_d^* = K_p \cdot (v_d^* - v_d) + K_i \cdot \int (v_d^* - v_d) \cdot dt \dots \dots \dots (13)$$

$$i_q^* = K_p \cdot (v_q^* - v_q) + K_i \cdot \int (v_q^* - v_q) \cdot dt \dots \dots \dots (14)$$

### 4.2.2 Current Control Loop

On the other hand, the current control loop uses the output of the voltage controller  $i_d^*$  and  $i_q^*$  as inputs as per equations 15 and 16.

$$v_d^* = K_p \cdot (i_d^* - i_d) + K_i \cdot \int (i_d^* - i_d) \cdot dt \dots \dots \dots (15)$$

$$v_q^* = K_p \cdot (i_q^* - i_q) + K_i \cdot \int (i_q^* - i_q) \cdot dt \dots \dots \dots (16)$$

## 4.3 Grid-Supporting Controller

### 4.3.1 Droop Control

A very small slope or gain (m and n) was chosen for the droop constants so that the change in frequency and voltage are reduced with respect to change in the load's active and reactive power.

$$\omega = \omega_{ref} - m \cdot (P - P_{ref}) \dots \dots \dots (17)$$

$$v_c = v_{c,ref} - n \cdot (Q - Q_{ref}) \dots \dots \dots (18)$$

Where,

$m$  = droop gain for frequency

$n$  = droop gain for voltage

### 4.3.2 Power Control Loop

The Power Control loop uses the output of the droop control as input. With the help of power equation ( $P=V \cdot I$ ) and the previous signal, the reference values for inner current control loop are obtained.

### 4.3.3 Current Control Loop

The current control loop uses the output of the power controller  $i_d^*$  and  $i_q^*$  as inputs as per equations 19 and 20.

$$v_d^* = K_p \cdot (i_d^* - i_d) + K_i \cdot \int (i_d^* - i_d) \cdot dt - \omega \cdot L_f \cdot i_q + v_{cd} \dots \dots \dots (19)$$

$$v_q^* = K_p \cdot (i_q^* - i_q) + K_i \cdot \int (i_q^* - i_q) \cdot dt - \omega \cdot L_f \cdot i_d + v_{cq} \dots \dots \dots (20)$$

## 5. Simulink Model

Two microgrids operating in parallel and feeding the resistive load through line impedances and breakers are shown in the figure 6 below.

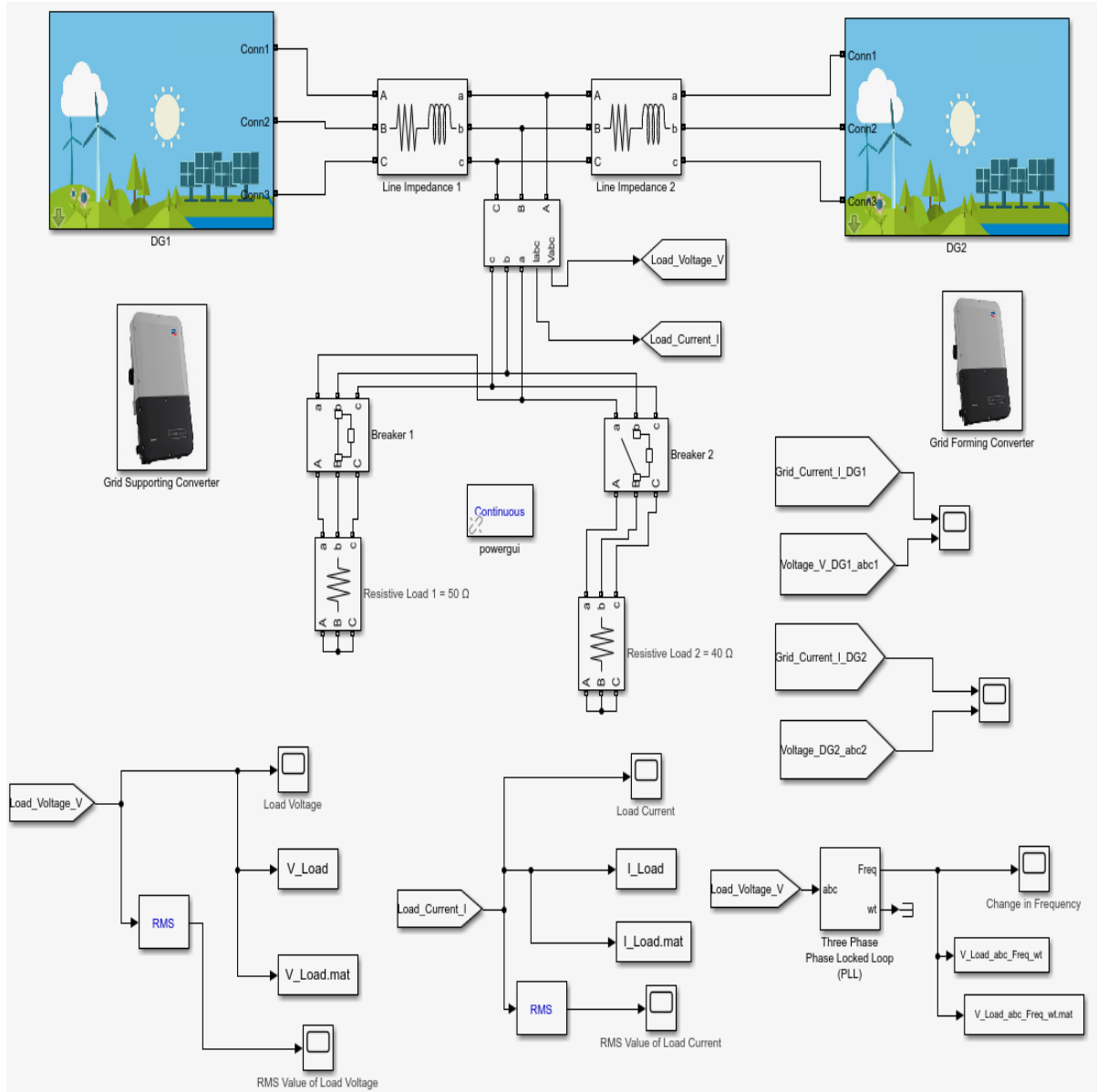


Figure. 6 Configuration for two microgrids operating in parallel and feeding load

According to the design specification, grid-supporting controller functioning as CSI is conforming the voltage of Grid-forming controller functioning as VSI. Until 0.2 seconds, the breaker 1 will be connected to the resistive load of 50  $\Omega$  and breaker 2 will be connected to other resistive load of 40  $\Omega$

after 0.2 seconds. After that, breaker 1 will be disconnected which helps to perform the small signal stability of the system.

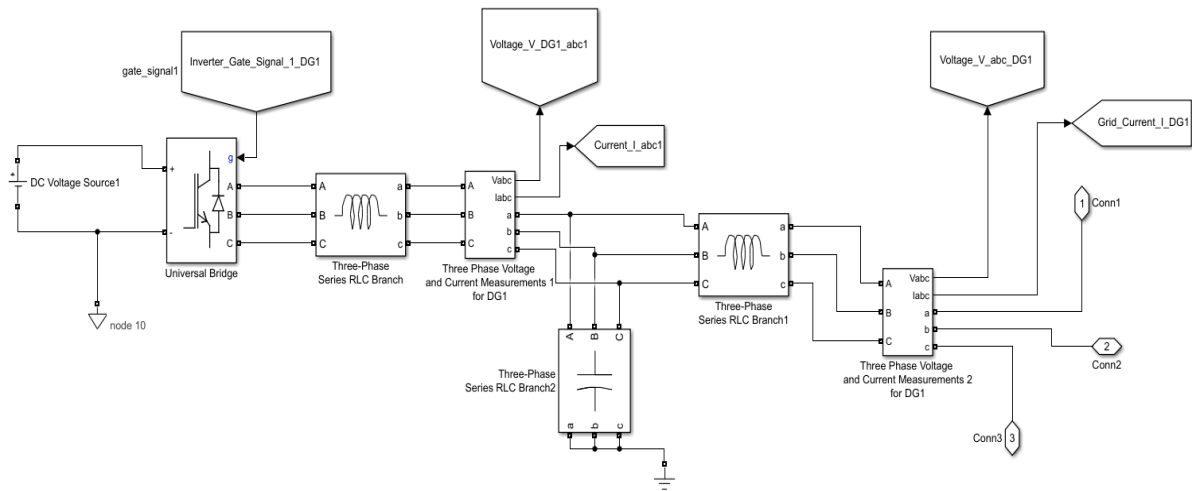


Figure. 7 Internal connection of Distributed Generator (DG1)

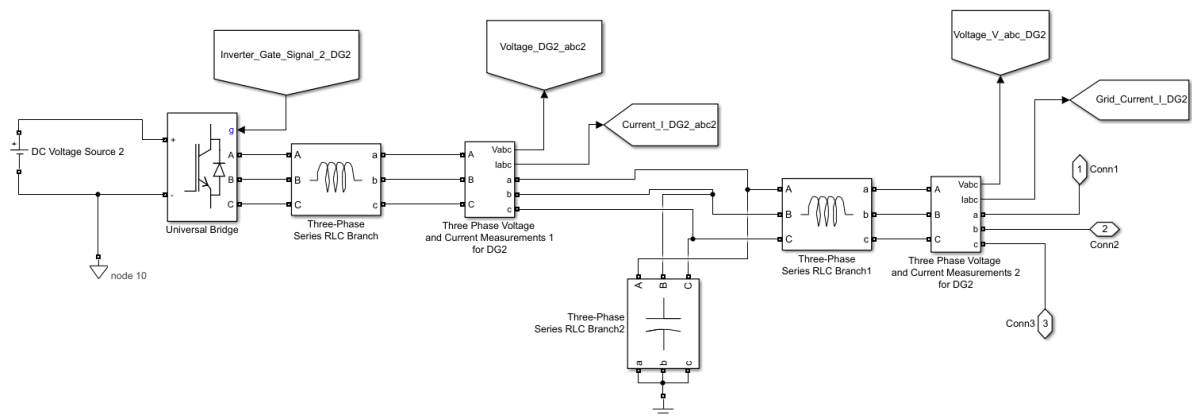


Figure. 8 Internal connection of Distributed Generator (DG2)

Figure. 7 and Figure. 8 illustrate the internal connection for DGs. Both generators are connected to a voltage source of 750V DC, inverters (Universal bridge) and three phase line.

Grid supporting controller functioning as CSI and Grid-forming controller functioning as VSI are shown in following figures.







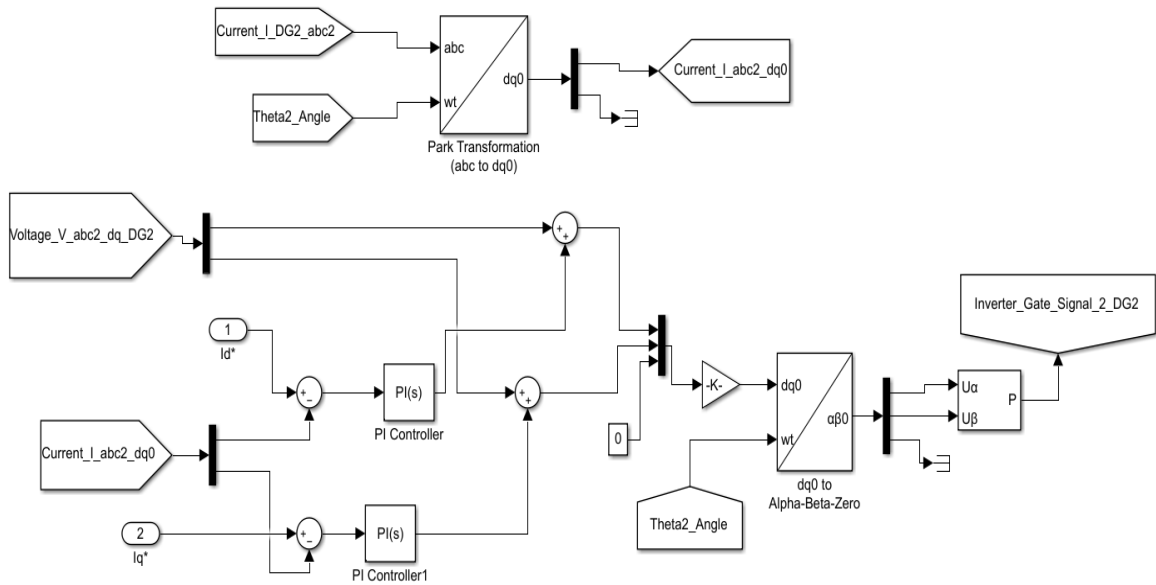


Figure. 14 Current Controller for Grid-forming Controller functioning as VSI

## 6. Simulation Result, Analysis and Conclusion

The following figure 15 demonstrate the value of d and q component of grid voltage due to changing load. Here, Demux4/1 signal is defined as  $V_d$  (blue color) and Demux4/2 signal is defined as  $V_q$  (red color). As we can see that  $V_d$  is showing pretty much constant value and  $V_q$  is zero.

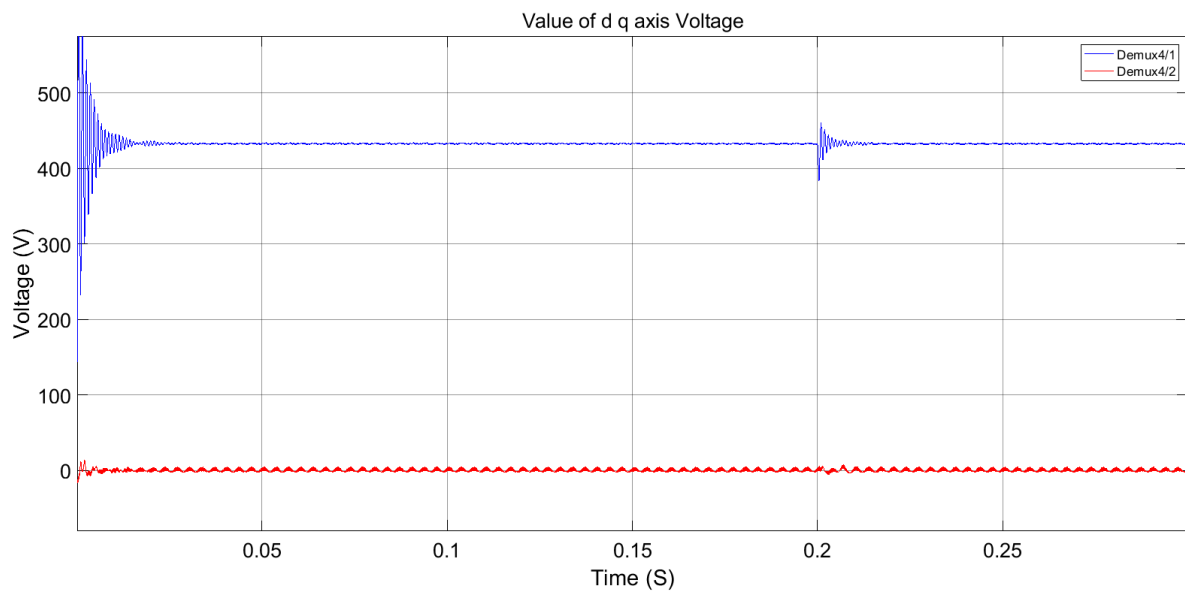


Figure. 15 Value of  $V_d$  and  $V_q$  components of Grid voltages with load shift

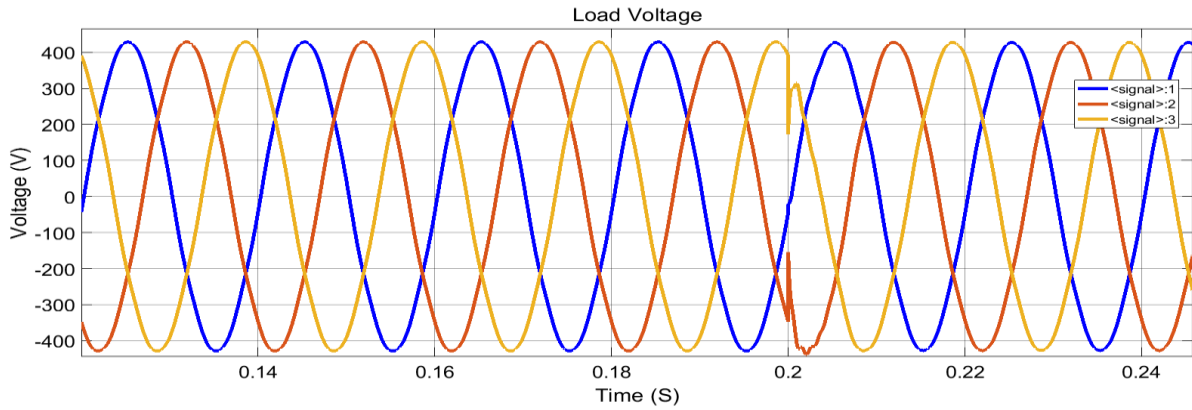


Figure. 16 Value of Three phase load voltage with load change

The above figure. 16 is showing the characteristics for variation in load voltages due to shift in load at 0.2 sec. Even though voltage affected only at 0.2 second due to load change, controller provides a constant output voltage.

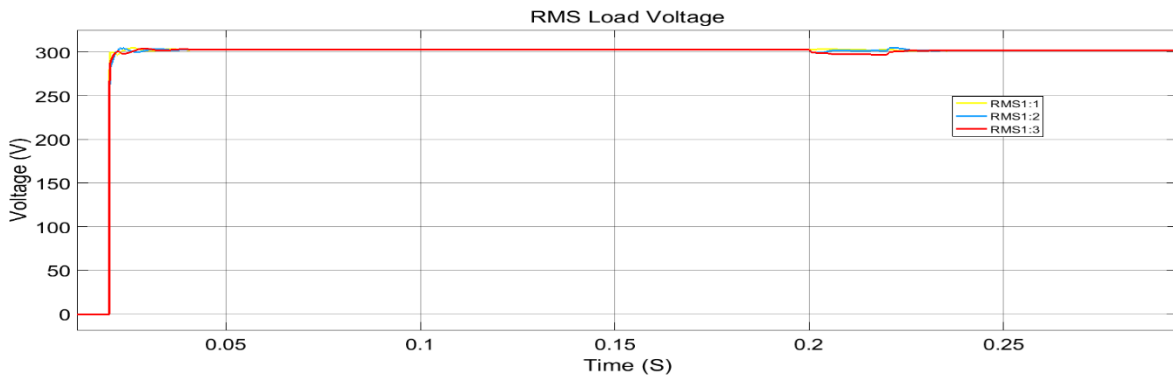


Figure. 17 RMS value of load voltage with change in load

The above figure. 17 presents the effect of load change on the value of RMS value of load voltage. There is not much deviation of voltage from the rated voltage. The value of the deviation is 2% which is within the allowed voltage deviation limit of  $\pm 10\%$ . Moreover, phase voltage is higher than the load voltage in this case as a result of reduction in line impedance.

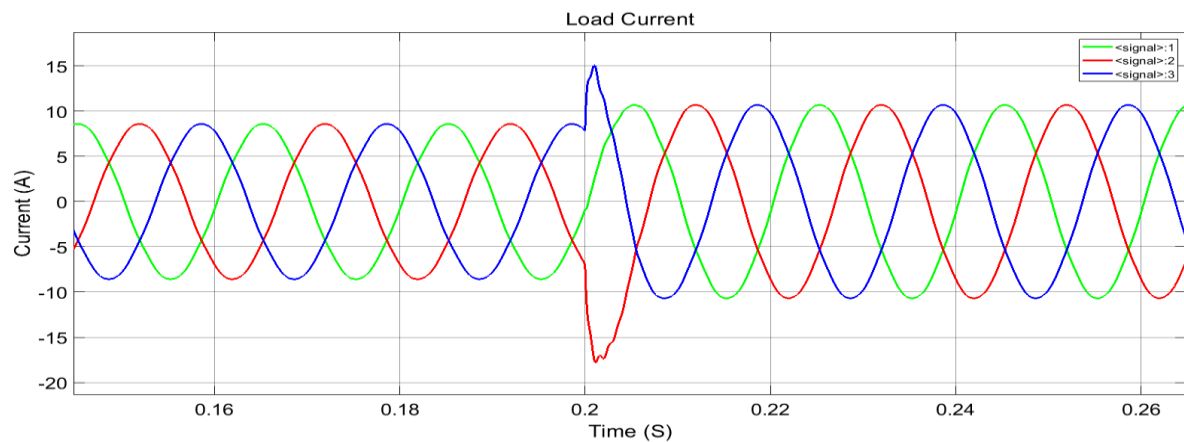


Figure. 18 Value of Three phase load current with load change

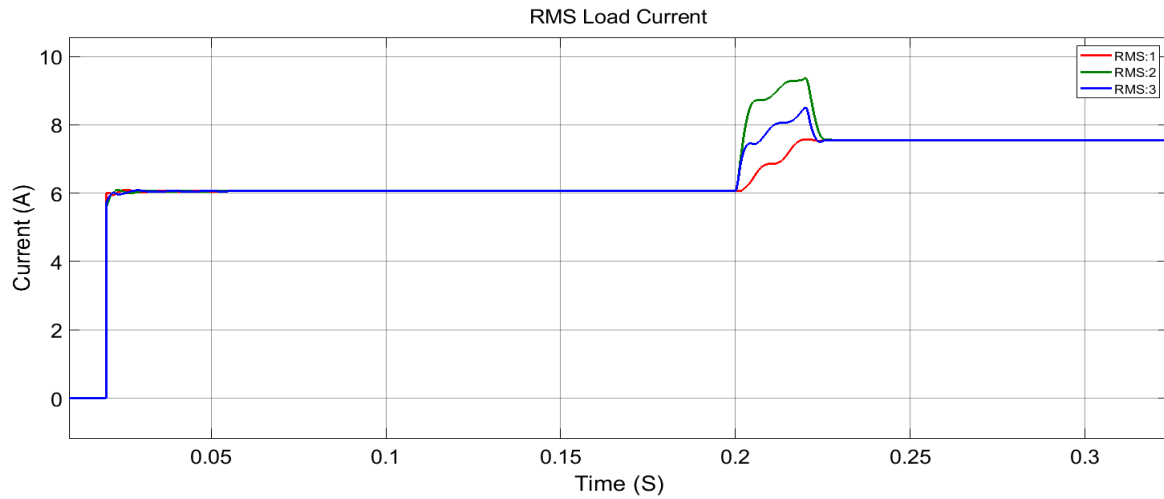


Figure. 19 RMS load current with load change

Variation of the load current and RMS value of the load current is shown in Figure .18 and Figure. 19. We observed that after load change at 0.2 sec, the value of both load current and RMS load current changed from their previous value and remained constant.

The following figure. 20 demonstrates the effect of change in load at 0.2 sec on the frequency. Although frequency deviate around 0.276% (frequency range 50.068-49.93) from the rated value, it is within the acceptable limit of  $\pm 3\%$ .

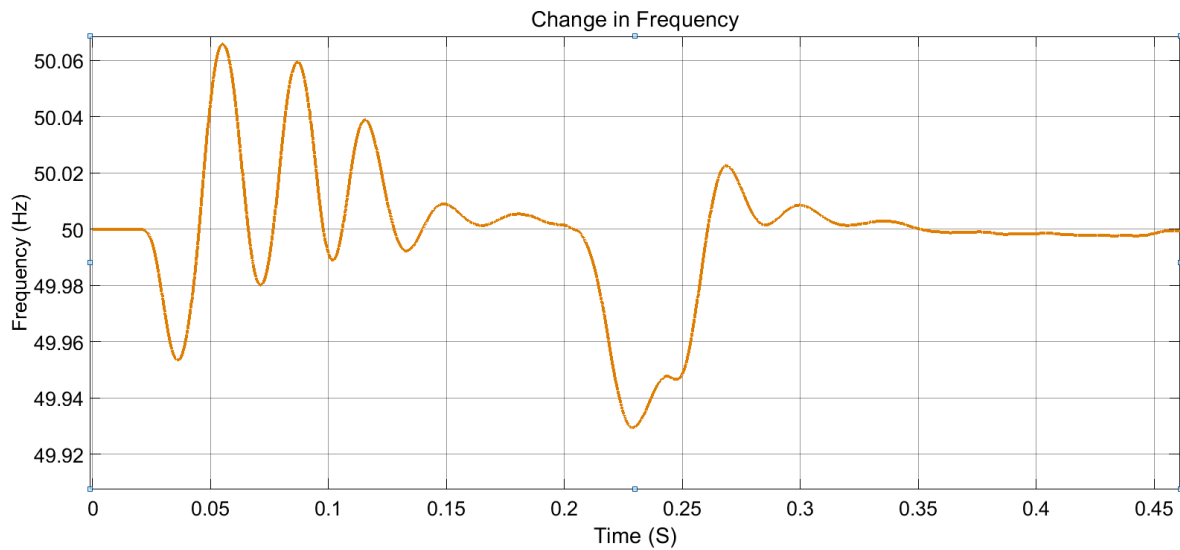


Figure. 20 Frequency deviation with load change

## 7. References

1. J. Rocabert, A. Luna, F. Blaabjerg and P. Rodríguez, "Control of Power Converters in AC Microgrids," in *IEEE Transactions on Power Electronics*, vol. 27, no. 11, pp. 4734-4749, Nov. 2012.
2. About Microgrids | Building Microgrid, 2019. [Online]. Available: <https://building-microgrid.lbl.gov/about-microgrids>. [Accessed: August 10, 2019].
3. Kalpesh C. Soni and Firdaus F. Belim, "MicroGrid during Grid-connected mode and Islanded mode - A Review," in *International Journal of Advance Engineering and Research Development (IJAERD)*, 2015. [Online]. Available: Oxford Reference Available: [http://www.ijaerd.com/papers/special\\_papers/EE22.pdf](http://www.ijaerd.com/papers/special_papers/EE22.pdf). [Accessed: August 10, 2019]
4. T. C. Green and M. Prodanovic, "Control of inverter-based micro-grids," *Electr. Power Syst. Res. Distrib. Generation*, vol. 77, no. 9, pp. 1204–1213, 2007.
5. A. Engler, "Control of inverters in isolated and in grid tied operation with regard to expandability in tutorial: Power Electronics for Regenerative Energy, " presented at the Proc. IEEE Power Electron. Spec. Conf., Aachen, Germany, 2004.
6. K. De Brabandere, B. Bolsens, J. Van den Keybus, A. Woyte, J. Driesen, and R. Belmans, "A voltage and frequency droop control method for parallel inverters, " *IEEE Trans. Power Electron.*, vol. 22, no. 4, pp. 1107–1115, Jul. 2007.
7. Lecture Notes on Power Electronics: Control, Synthesis, Application; Univ.-Prof. Dr. R.W. De Doncker; ISEA RWTH University.
8. Abbas, S. Z. (2016). Simulation, Implementation and Testing of Three-phase Controlled Power Inverter Behavior (Master thesis).
9. Poh Chiang Loh and D. G. Holmes, "Analysis of multiloop control strategies for LC/CL/LCL-filtered voltage-source and current-source inverters," in *IEEE Transactions on Industry Applications*, vol. 41, no. 2, pp. 644-654, March-April 2005.
10. Lecture Slides, Converter Control and Microgrid: Univ.-Prof. Dr. Antonello Monti; Automation of Complex Power Systems; E.ON Energy Research Center.